

Efficient removal of Pb^{2+} , Ni^{2+} Cu^{2+} , and Zn^{2+} ions from water using activated soybean seed adsorbent

F. Ummul Khair^{1*}, N. Gulrez¹, H. Mohd Kamil²

¹Department of Chemistry, Sir Syed Faculty of Science, Mohammad Ali Jauhar University, Rampur 244901, India

²Department of Chemistry, Govt. Raza P.G. College, Rampur 244901 (MJP Rohilkhand University Bareilly) India

Received: March 2023; Revised: August 2023

Industries often release contaminated water containing various pollutants, including hazardous heavy metals, posing significant risks to the environment. To mitigate these dangers, effective water treatment methods are essential. Adsorption is a well-established, cost-effective process for water treatment. In this research, we investigated the use of activated soybean seed (ASS) as an adsorbent for removing heavy metal ions from waste water. Batch experiments were conducted to assess the efficiency of ASS in removing Pb^{2+} , Ni^{2+} Cu^{2+} , and Zn^{2+} . The study examined the impact of several parameters, such as pH, adsorbent dose, shaking time, shaking speed, temperature, and particle size, on the adsorption rate. The equilibrium data were fitted using the Langmuir, Freundlich, and Temkin adsorption isotherm models, while the kinetic data were analyzed using the pseudo-first-order (PFO) and pseudo-second-order (PSO) kinetic models. To understand the changes occurring during the adsorption process, we characterized the ASS adsorbent before and after adsorption using SEM, XRD, TGA, ICP-MS, and FT-IR spectrometry. This study provides valuable insights into the potential application of activated soybean seed as an effective adsorbent for heavy metal removal from aqueous solutions.

Keywords: Soybean seed, adsorbent, heavy metal, waste water.

INTRODUCTION

Pollution is the presence of unwanted substances, known as pollutants, in the environment, surpassing allowable contaminant limits and negatively impacting all aspects of life. Water contamination arises not only from man-made sources like rapid industrialization and the excessive use of chemicals such as hydrocarbons, heavy metals, chlorinated hydrocarbons, and pesticides, but also from natural factors like geothermal activities, space dust, and volcanic eruptions [1,2]. It is worth noting that man-made sources are the primary contributors to pollution in comparison to natural ones [3]. Heavy metals like As, Cd, Hg, and Pb are well-known for their toxicological manifestations and the harm they can cause [4, 5]. Heavy metals, including As, Cd, Hg, and Pb, pose significant threats to the aquatic environment and the food chain, even at low concentrations [6, 7]. These heavy metals are non-biodegradable, leading to their widespread presence in the environment. Their accumulation can result in various irreversible health effects [8, 9]. Many biological processes, membrane processes, sedimentation, ion-exchange, chemical reduction, electro-desposition, and adsorption have their benefits and application limitations. While the adsorption process is an environmental-friendly

[10], low-cost, easy method, effective-purification, and separation technique, used in industry for the removal of contaminated water [11]. This facilitates availability and makes the process cost-effective, as non-living biomass requires no maintenance or nutrient input [12, 13].

The efficient recovery of heavy metals from living biomass is challenging due to their tight binding within the cell structure. As a result, residual soybean biomass serves as a promising adsorbent, benefiting from its abundance and favorable physicochemical properties [12]. This study aims to assess the effectiveness of soybean adsorbents in removing Pb^{2+} , Ni^{2+} Cu^{2+} , and Zn^{2+} ions from aqueous solutions. Batch studies were conducted, exploring various parameters such as adsorbent dose, pH, shaking time, shaking speed, temperature, and particle size, to investigate the adsorption of Pb^{2+} , Ni^{2+} Cu^{2+} , and Zn^{2+} by soybean. The equilibrium data were analyzed using several isothermal models. The research endeavors to evaluate a novel, cost-effective biosorbent suitable for environmental applications.

MATERIALS AND METHODS

Preparation of adsorbent

Soybean seeds were collected from Rajasthan, India, followed by washing with distilled water and

* To whom all correspondence should be sent:
E-mail: ummulkhairfatma@gmail.com

sun-drying for about 3-5 days before grinding. Later on seeds were ground into small particles by using a manual grinder then fine particles were classified into three particle sizes: 300 μm , 355 μm and 710 μm . The soybean powder particles were subjected to treatment using NaOH solutions with concentrations of 0.5%, 1%, and 1.5% to create a negative control. Subsequently, the soybean powder slurry obtained was dried in an oven at 75°C for 3 hours and stored in a container for future use. For study the standard stock solution of Pb^{2+} , Ni^{2+} , Cu^{2+} , and Zn^{2+} were prepared by dissolving suitable Pb (CH_3COOH)₂ · 3H₂O, CuSO₄ · 5H₂O, ZnCl₂, and NiCl₂ · 6H₂O in distilled water. All chemicals used were analytical reagent grade for the experiments. Distilled water was used for the experiments.

Characterization of ASS adsorbent

The characterization of the treated and untreated ASS was done by using FT-IR, SEM, ICP-MS, XRD, and TGA. Surface morphology and texture of the adsorbent was observed by using SEM and FT-IR analysis was used to determine the functional groups and sites in the ASS at the range of 4000 to 400 cm^{-1} . Structures and phases of before and the after adsorption of ASS adsorbent

surfaces were examined using a XRD at a 2 θ diffraction angle of 5° to 80° with the scan rate was 10/min. The characterization of thermal degradation of untreated and treated adsorbent was performed using TGA. The analysis of adsorbent was determined by using ICP-MS.

RESULTS AND DISCUSSION

Characteristics of the adsorbents Scanning electron microscope analysis

The SEM analysis was used to characterize the surface morphology of the ASS adsorbents before and after the adsorption of metal ions (Figure 1 a-f). The surface of the ASS adsorbent significantly changes after the interaction with metal ions. Prior to adsorption, the ASS exhibited a visibly smooth surface texture with distinct particles of different sizes on its surface. However, after interacting with Pb^{2+} , Ni^{2+} , Cu^{2+} , and Zn^{2+} ions, the morphology of the ASS adsorbent underwent a transformation, leading to the presence of rougher stone particles with increased size. This change suggests that Pb^{2+} , Ni^{2+} , Cu^{2+} , and Zn^{2+} ions were efficiently absorbed on the ASS surface, indicating the active sites' capacity to adsorb these metal ions to the maximum extent [13,14].

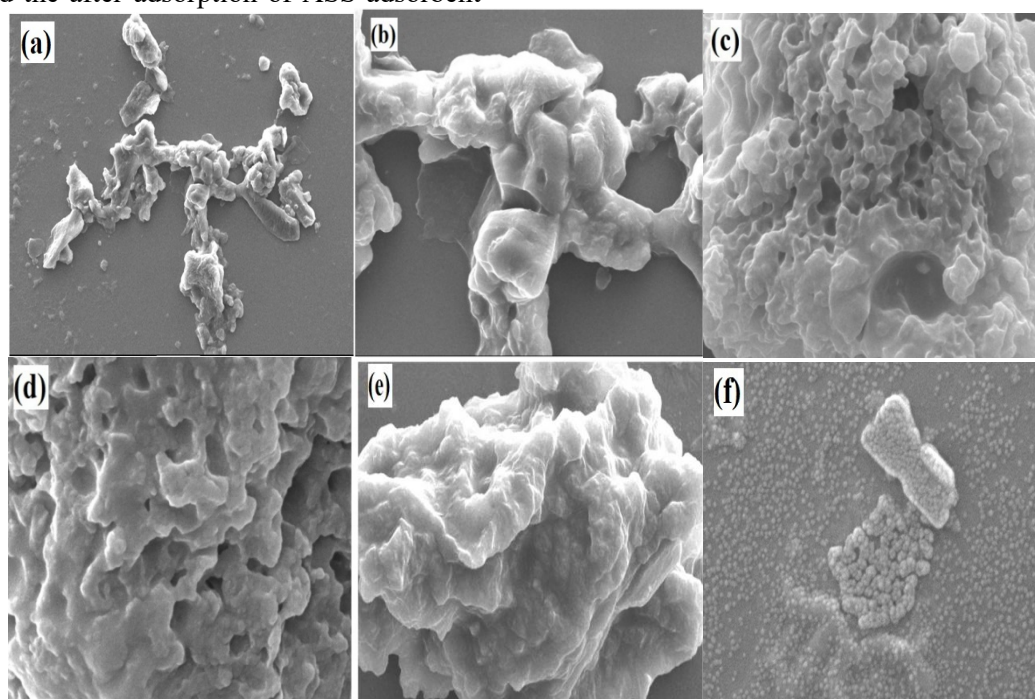


Fig. 1. SEM image of ASS adsorbent (a) & (b) before adsorption (c), (d), (e), (f) after adsorption of Cu^{2+} , Pb^{2+} , Zn^{2+} , Ni^{2+}

Fourier transform infrared spectroscopy analysis (FTIR)

FTIR analysis was conducted to examine the functional groups present on the surface of the ASS adsorbent before and after the adsorption of heavy metal ions. The analysis also revealed functional groups associated with the binding of metals to the adsorbent (Fig. 2a). The FTIR peaks in cm^{-1} of the ASS sample exhibited a strong and broad band between 3200 and 3500, indicating the presence of the O-H group. Additionally, two adsorption peaks at 2924 and 2856 were assigned to alkyl (-C-H) groups. Other absorption bands were observed at 1746, 1646, and 1454, which corresponded to the stretching vibrations of the carbonyl group (-C=O)

and -C-O from the carboxyl group. The peak at 1540 represented the N-H bending vibration of the amine group, while the C-N stretching was observed at 1247. The C-O stretching vibration was noticed at the 1054 absorption band. Upon adsorption of heavy metal ions, the absorption peaks of the OH group, C-N, and C-O stretch shifted. Specifically, the absorption band of the -OH group changed from 3362 to 3288, 3298, 3392, and 3492 when interacting with Pb^{2+} , Ni^{2+} , Cu^{2+} , and Zn^{2+} respectively. Similarly, for the C-N stretching vibration, peaks shifted from 1240 to 1242, 1240, 1244, and 1244 respectively for Pb^{2+} , Ni^{2+} , Cu^{2+} , and Zn^{2+} . The FTIR analysis indicated that hydroxyl groups and amine groups serve as major adsorption sites in the ASS adsorbents [13, 15].

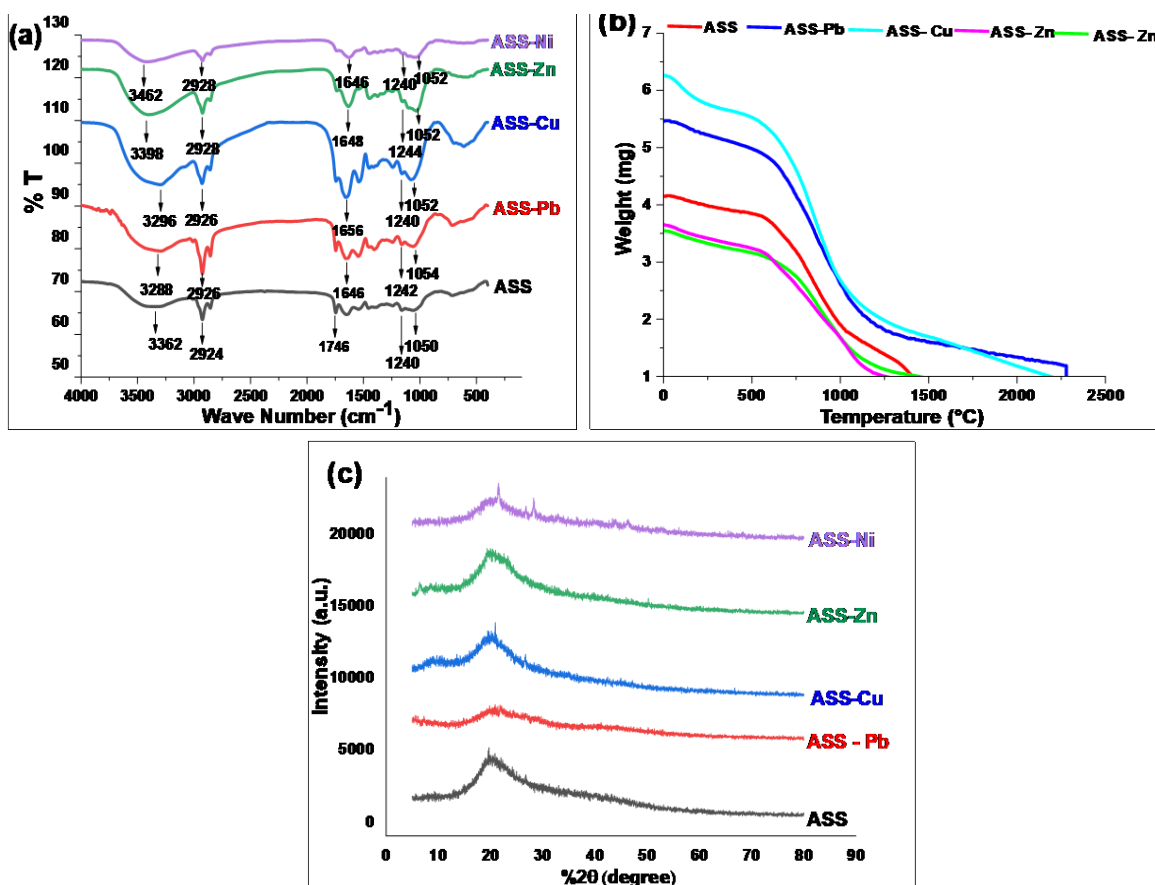


Fig. 2. (a) FT-IR spectra of ASS adsorbent, sample ASS-Pb, ASS-Cu, ASS-Zn and ASS-Ni. (b) TGA for original ASS adsorbent, sample ASS-Pb, ASS-Cu, ASS-Zn and ASS-Ni. (c) XRD for original ASS adsorbent, sample ASS-Pb, ASS-Cu, ASS-Zn and ASS-Ni

Thermogravimetric analysis (TGA)

TGA was employed to study the thermal degradation of the adsorbent before and after metal deposition. This technique allows for the assessment of the material's thermal stability in a controlled atmosphere and measures the rate of weight change

as a function of time and temperature. TGA is commonly used to determine the compositional properties, as well as the thermal and oxidative stability of materials [13]. For the analysis, approximately 5.471 mg samples of the ASS adsorbent were subjected to heating from $30^{\circ}C$ to $800^{\circ}C$, with the temperature gradually increased at a

rate of 20°C/min (Fig. 2b). The changes in weight loss of the ASS adsorbent concerning temperature and time were observed using TGA.

X-ray diffraction analysis (XRD)

XRD of ASS adsorbent before and after Pb^{2+} , Ni^{2+} , Cu^{2+} , and Zn^{2+} adsorption are also analyzed at 2θ at a diffraction angle of 5° to 80° . The scan rate was 10°C/min. This analysis method gave information about the crystal structure of ASS. However, a decrease in peak density after Pb^{2+} adsorption is indicative of the decreasing degree of crystallinity [16]. Fig. 2c shows that there are no significant peaks for Pb^{2+} , Ni^{2+} , Cu^{2+} , and Zn^{2+} in the loaded ASS samples, indicating that ASS adsorbent surface is amorphous before and after adsorption. Amorphous solids are good adsorbents, having more active sites and higher specific surface area. So, ASS was observed to be an effective adsorbent for the adsorption of Pb^{2+} , Ni^{2+} , Cu^{2+} , and Zn^{2+} from contaminated water.

Study of pH of metal ion solutions

The value of pH of the solution is important parameter, affecting the adsorption of metal ions by ASS. The pH of metal ion solutions is investigated in the range of 3-8 and pH is adjusted by NaOH and HCl. Elimination efficiency of metal ions is depends on the concentration of hydrogen ions present in an aqueous solution. It was observed for all metal ions studied, the adsorption decreases with decreasing pH beyond 5. The decrease in metal ions adsorption at low pH can be responsible for contesting between metal ions and H^+ ions. Therefore, it is clear from fig. 3a that at a low pH, the adsorption of the studied metal ions is significantly reduced. Though, with a continuous increase in pH, the adsorption rate may decrease due to metal hydroxide formation. So, the optimum pH value of 5 was chosen for further study. According to the results, the removal rate of metal ions increases with increasing pH up to a certain limit, beyond pH 6 the rate of removal of metal ions decreases gradually. It was observed that at lower pH, the active sites were taken by protons on the ASS surface. [3, 16, 17].

Study of adsorbent dose of adsorbent on adsorption

The effect of the adsorbent dose is noteworthy parameter to the adsorption of metal ions from an aqueous solution. This experiment was carried out at different adsorbent doses from 1 to 6 g/100ml, optimal pH (3-6), 4 h shaking speed, and 28 °C temperature (fig. 3b). According to the results, it was found that the rate of adsorption of metal ions

increases by the increase in adsorbent dose due to the presence of active sites for adsorption [13, 15]. The maximum removal of Pb^{2+} , Cu^{2+} , Zn^{2+} , and Ni^{2+} was shown at 4g/100ml by ASS adsorbent from 61.07% to 86.15%, 26.69% to 60.70%, 33.92% to 68.34% and 24.54 % to 69.82%, respectively. Further, the increase ASS adsorbent dose from 4 to 6 g/100ml then the adsorption of the Pb^{2+} , Cu^{2+} , Zn^{2+} , and Ni^{2+} decreased from 86.15% to 85.71%, 60.70% to 59.37%, 68.34% to 58.88% and 24.54% to 67.24, respectively. This may be due to the overlap of the adsorption site and the crowding of adsorbent particles [3, 18].

Study of the shaking time of the aqueous solution of heavy metal with the ASS adsorbent

In this experiment, the effect of contact time was conducted at 25-28 °C by the different adsorption time from 1 to 4 h (Fig. 3c). The adsorption of metal ions increases with increasing contact time [13] but remained suitable after reaching equilibrium [19]. The maximum adsorption percent of Pb^{2+} , Cu^{2+} , Zn^{2+} , and Ni^{2+} was obtained at a 3h shaking time. Then after a while, it reaches an equilibrium state after which the amount of adsorption does not increase significantly.

Study of the shaking speed of the aqueous solution of heavy metal with the ASS adsorbent

The effect of shaking speed on the removal of metal ions was investigated by ASS adsorbent at different shaking speeds of 220 and 320 rpm. This experiment was carried out at adsorbent doses from 4g/100ml, optimal pH (3-6), and 4h shaking speed. At 220 rpm shaking speed the adsorption of Pb^{2+} , Cu^{2+} , Zn^{2+} , and Ni^{2+} metals were found to be 94.87%, 58.22%, 63.78%, & 76.43%, respectively. However at 320 rpm shaking speed the adsorption of Pb^{2+} , Cu^{2+} , Zn^{2+} , and Ni^{2+} were found to be 78.7%, 51.41%, 59.33% & 54.98%, respectively. Fig. 3d indicates that the percent removal of heavy metal ions increased at decrease in shaking speed and obtained maximum adsorption of metal ions at near 220 rpm. Adsorption of heavy metal ions was found less than optimum at lower and higher shaking speeds. The low shaking speed could not sufficiently disperse the particles in water to provide active binding sites for metal ions adsorption. On the other hand, the high shaking speed strongly dispersed the AAS particles in the water and did not give them enough time to bond with the metal ions.

Study of the temperature of the heavy metal solution with the adsorbent

The adsorption capacity of ASS for removal of metal ions was investigated at the various temperature of 25-50 °C with adsorbent dose 4g (Fig.3e). In addition, temperature directly affects the reaction rate between adsorbate and adsorbent in an aqueous solution during the adsorption process. The diffusion rate of adsorbed molecules increases with increasing temperature from the outer boundary layer to the pores of the adsorbent. This can lead to

a decrease in the viscosity of the solution [20]. Maximum adsorption of Pb^{2+} , Cu^{2+} , Zn^{2+} , and Ni^{2+} was observed at 35°C and decreased with a further increase in temperature. This may be due to the deterioration of the solution's ion balance, the destruction of active binding sites in the residual AAS, or the increased tendency to separate metal ions from the solution interface [13]. The mobility of metal ions increases with increased temperature; it is recommended that the adsorption is endothermic in nature [21].

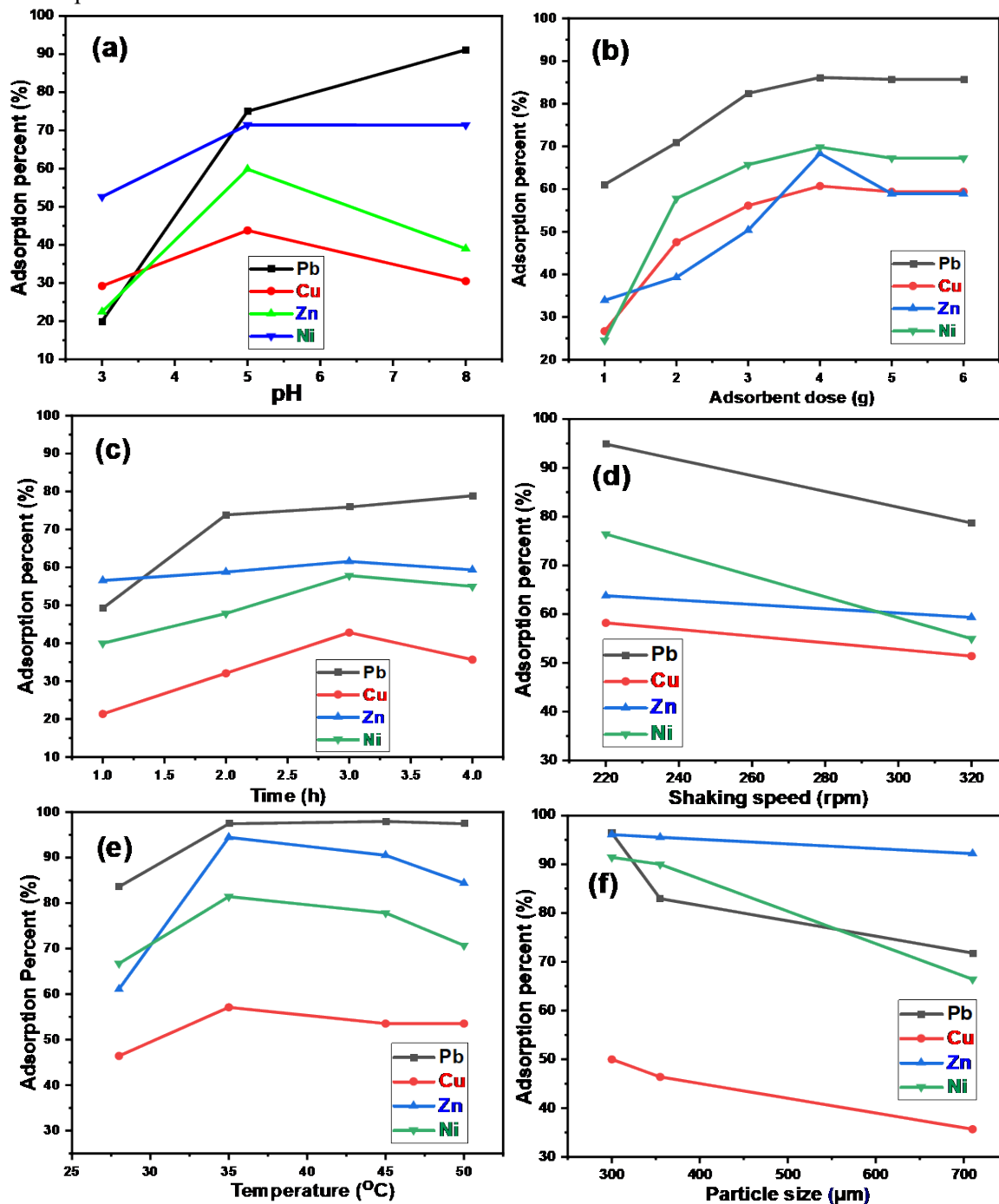


Fig. 3. (a) Effect of pH; (b) Effect of adsorbent dose; (c) Effects of shaking time; (d) Effects of shaking speed; (e) Effects of temperature; (f) Effects of particle size

Study of particle size of adsorbent on adsorption

The effect of adsorption by particle size was studied from several surface areas of various particle sizes of ASS adsorbent. The adsorption capacity of ASS for the removal of Pb²⁺, Cu²⁺, Zn²⁺, and Ni²⁺ was investigated at various particle sizes 300, 355, and 710 μm with adsorbent dose 4g (Fig. 3f). As shown, the adsorption capacity of the heavy metals decreases with increases in the adsorbent particle size from 300μm < 710 μm, the percent adsorption of Pb²⁺, Cu²⁺, Zn²⁺, and Ni²⁺ was decreasing from 96.41 to 71.79%, 50 to 35.66%, 96.1 to 92.19% and 91.42 to 66.42%, respectively.

Thermodynamic parameters and temperature distribution

In this study, the effect of temperature on the adsorption of ASS for the removal of metal ions was investigated at 301, 308, 318, and 328K temperatures. The nature of adsorption of exothermic or endothermic, spontaneity, and feasibility was evaluated by thermodynamic parameters of Gibbs energy (ΔG°), entropy (ΔS°), and enthalpy (ΔH°). Values of thermodynamic parameters calculated as a function of temperature changes are given in Table 2. According to this

study, the value of ΔS° was found to be positive at tested 301, 308, 318, and 328K temperatures and ΔH° was also found to be positive. The system is endothermic due to the positive value of ΔH°. Adsorption is the spontaneous process or not, dependent on Gibbs energy. The negative value of Gibbs energy indicates, the adsorption process is a spontaneous process.

C_i and C_e are the initial and equilibrium concentrations of metal ions Pb²⁺, Cu²⁺, Zn²⁺ and Ni²⁺ (mg/L) respectively in an aqueous solution. m – Mass (g). R is gas constant (8.314 J mol⁻¹ K⁻¹). T is absolute temperature (K). V is volume of heavy metal ion solution. k_d is adsorption affinity. Enthalpy (ΔH), entropy (ΔS). Gibbs free energy (ΔG⁰). k₁ is a PFO rate constant. k₂ is PSO rate constant. K_f is Freundlich isotherm constant. 1/n is the adsorption intensity. q_e the amount of adsorbed metal per gram of the ASS adsorbent at equilibrium (mg g⁻¹). ‘a’ is the equilibrium binding constant and ‘b’ represents the intensity of adsorption. K_T is Temkin constant. q_{max} is maximum adsorption capacity (mg g⁻¹). K_L is Langmuir isotherm constants (L mg⁻¹). Adsorption of Pb²⁺, Cu²⁺, Zn²⁺ and Ni²⁺ are decreased at high temperature and also the value of ΔG⁰ is decreased with increased temperature

Table 1. Equations used in Pb²⁺, Cu²⁺, Zn²⁺, and Ni²⁺ adsorption isotherm on ASS.

Isotherm	Equation	Equation No.
Adsorption capacity	$q_e = (C_i - C_e) \frac{V}{W}$	1
Adsorption yield	$R\% = \frac{(C_i - C_e)}{C_i} \times 100$	2
Langmuir	$\frac{1}{q_e} = \frac{1}{k_L q_{max} C_e} + \frac{1}{q_{max}}$	3
	$R_L = \frac{1}{1 + C_i \times K_L}$	4
Freundlich	$Log q_e = Log K_f + \frac{1}{n} Log C_e$	5
Temkin	$q_e = a + b log C_e$	6
PFO	$ln(q_e - qt) = ln q_e - K_1 t$	7
PSO	$\frac{1}{q_t} = \frac{1}{k_2 q_e^2} + \frac{t}{q_e}$	8
Thermodynamic studies	$\Delta G^\circ = -RT ln K_d$	9
	$ln K_d = \frac{\Delta S^\circ}{R} - \frac{\Delta H^\circ}{RT}$	10

Adsorption isotherms and kinetics

The adsorption isotherm model describes the relation between adsorbents and heavy metal ions in the solution at equilibrium state [22]. Pb^{2+} , Cu^{2+} , Zn^{2+} and Ni^{2+} adsorption study was conducted under the most favorable conditions. This study evaluated the adsorption behaviors and efficiency of ASS for Pb^{2+} , Cu^{2+} , Zn^{2+} and Ni^{2+} adsorption with the Langmuir, Freundlich, and Temkin isotherm models (Table 1). In Langmuir isotherm model, there is no interaction between the solute concentrations on the adsorbent surface. In this adsorption isotherm, absorption takes place on a homogeneous surface by monolayer absorption without interaction between adsorbed metal ions [13, 23]. The Freundlich isotherm model is assumed as a heterogeneous adsorbent surface that represents the interaction between the metal ions on the surface of the adsorbent and the metal ions concentration in the liquid [24]. The adsorption rate of heavy metal ions is equal to the rate of desorption of the same heavy

metal ions before the adsorption equilibrium occurs [25, 26]. Accordingly, the R^2 value was calculated from experimental data and concluded that Langmuir isotherm was the most favorable model for soybean adsorbent. As the results of the experiment R^2 values occur in Langmuir > Freundlich > Temkin order (fig.4 (a-d)). The data were fitted by the linear form C_e/q_e versus C_e , at a concentration range from 0.05 to 2g/l. The q_{max} and RL were calculated by slope and intercept, respectively. The results obtained with soybean adsorbent are consistent with previous batch adsorption studies [27, 28]. According to this kinetic adsorption model, PFO and PSO were used for Pb^{2+} , Cu^{2+} , Zn^{2+} and Ni^{2+} adsorption (Table 1). The value of coefficients (R^2) is shown in Table 2 with velocity and other constants. According to this study, the correlation coefficients were obtained 0.97294, 0.54588, 0.99674 and 0.97536 for the elimination of Pb^{2+} , Cu^{2+} , Zn^{2+} , and Ni^{2+} from aqueous solution by AAS. The intercept values of the lines drawn in Fig. 5(a-d) were used to determine the adsorption rate.

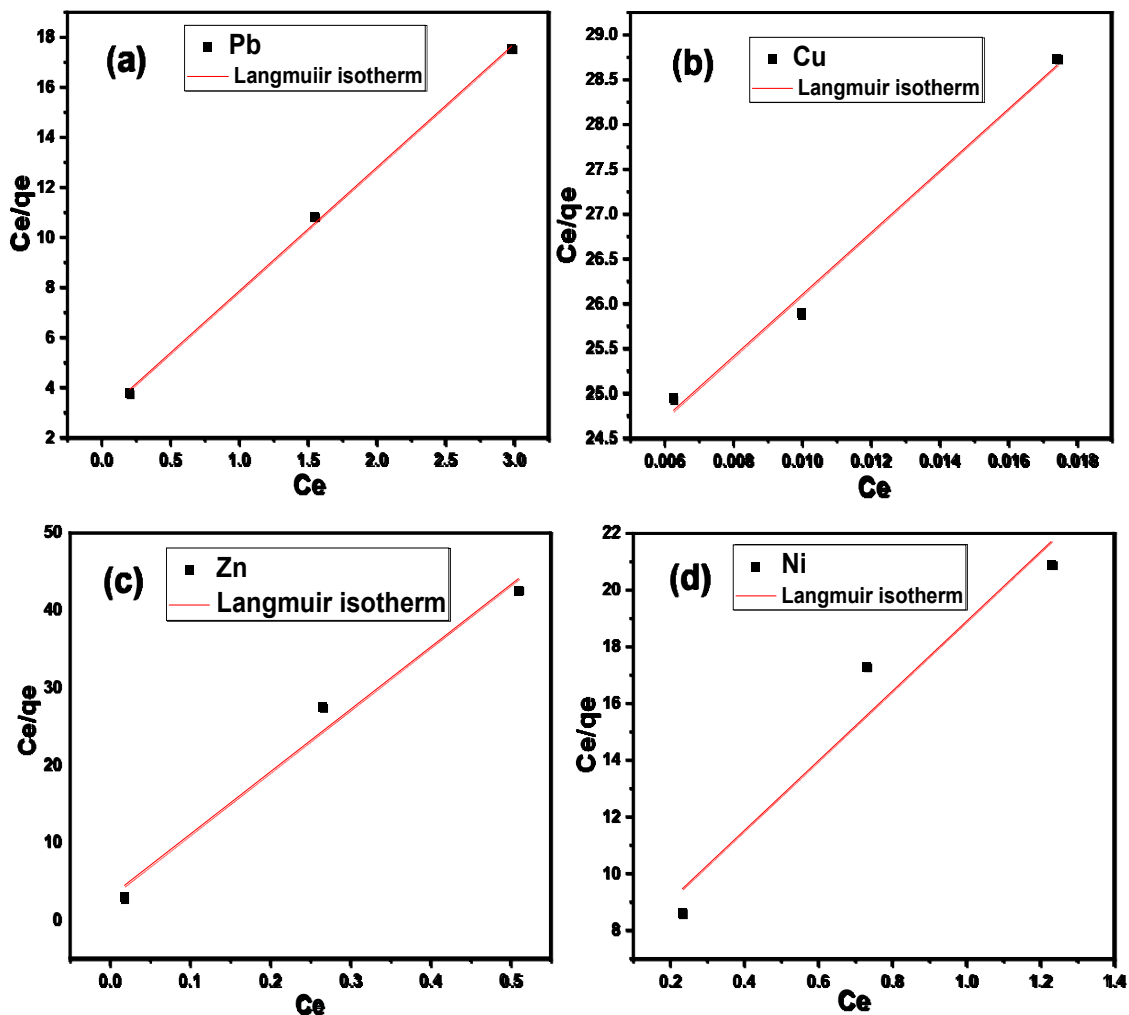


Fig. 4. Langmuir adsorption isotherms of (a) Pb^{2+} ; (b) Cu^{2+} ; (c) Zn^{2+} ; (d) Ni^{2+}

Based on the kinetic studies, it is clear that the rate of adsorption can be well described by a PSO. In other words, the data fit well with the proposed pseudo-quadratic equation. The data also showed that the initial metal ion concentration affected the

contact time required to reach equilibrium. The adsorption capacity increases for the highest initial concentrations of metal ions. These results show similarity to previous studies.

Table 2. Equations used in Pb^{2+} , Cu^{2+} , Zn^{2+} , and Ni^{2+} adsorption process on ASS adsorbent.

S.No.	Isotherms	Parameters	Values			
			Pb	Cu	Zn	Ni
1.	Langmuir	q_{max} (mg/g)	0.0698	0.0441	0.3429	0.1516
		K_L (l/mg)	0.0698	0.0001	0.0042	0.0123
		R_L	1.5083	1.000003	1.0027	1.0299
		R^2	0.9976	0.9838	0.9651	0.8915
2.	Freundlich	K_f	0.1121	0.0200	0.013	0.0517
		$1/n$	0.4462	0.8620	0.1816	0.4548
		R^2	0.9852	0.9974	0.9563	0.9681
3.	Temkin	a	0.0919	0.0037	0.001	0.0257
		b	0.2916	77.141	2832.86	3.7892
		R^2	0.6062	0.7072	0.8958	0.9256
4.	PFO	q_e	0.3514	0.0350	0.0306	0.1605
		K_1	-0.3452	-0.5098	-0.4185	-0.3093
		R^2	0.7810	0.5833	0.2580	0.5238
5.	PSO	q_e	0.15059	0.0002	0.0098	0.0352
		K_2	0.0126	0.000029	0.00016	0.00039
		R^2	0.9673	0.7963	0.9983	0.9753
6.	Thermodynamic studies	ΔH° (kJ/mol)	68.14	3.70	12.95	4.23
		ΔS° (J/mol/K)	214.11	14.29	96.29	5.31
		ΔG°_{301} (kJ/mol)	5.9595	1.1968	8.2867	8.2867
		ΔG°_{308} (kJ/mol)	1.0197	1.7443	3.6664	5.6610
		ΔG°_{318} (kJ/mol)	1.4206	0.42934	5.2900	6.4290
		ΔG°_{323} (kJ/mol)	7.2594	0.2584	7.4805	7.5396

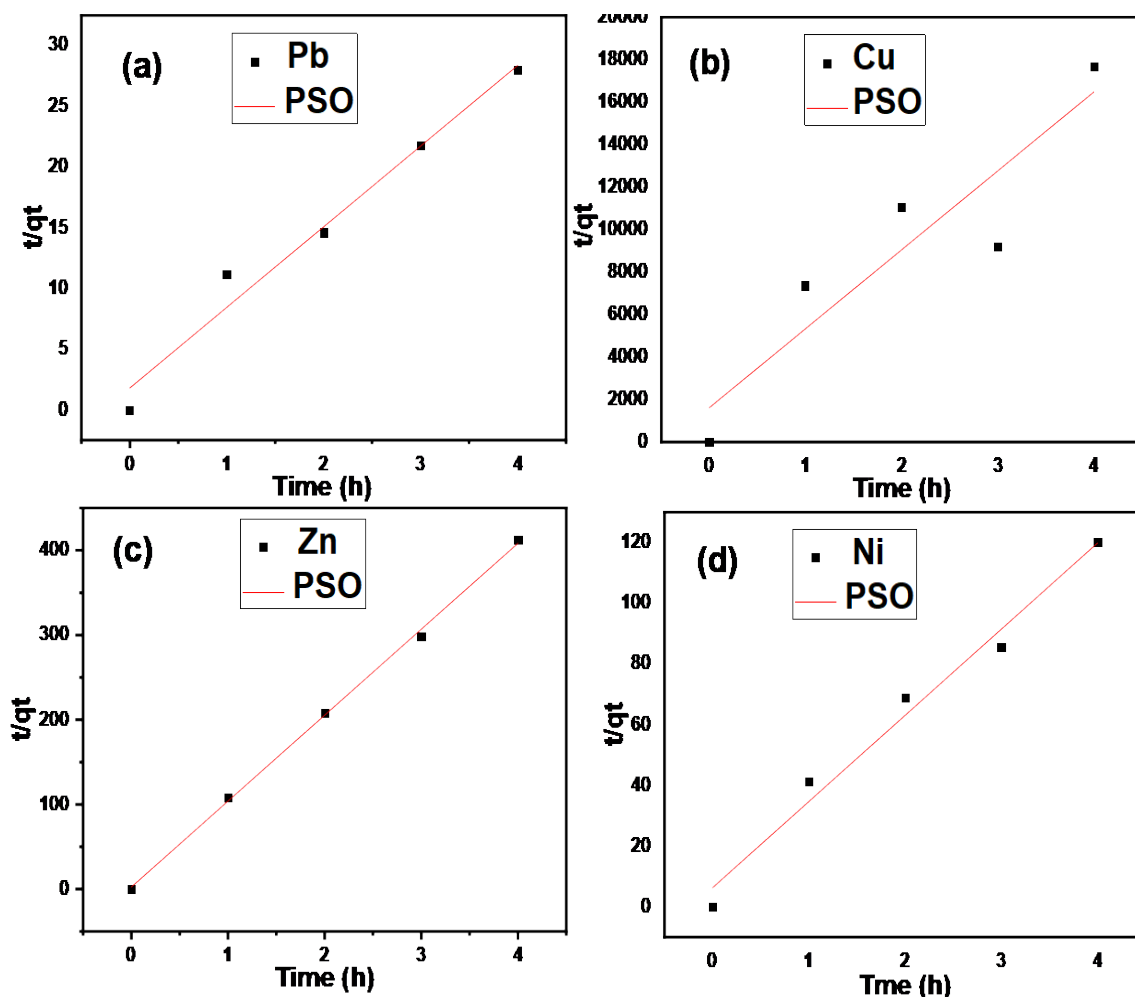


Fig. 5. PSO kinetic model of (a) Pb^{2+} ; (b) Cu^{2+} ; (c) Zn^{2+} ; (d) Ni^{2+}

CONCLUSION

Adsorption shows selectivity and higher efficiency in the elimination of heavy metals and also does not produce any pollutants. It is not only a low-cost but a highly effective process. Results of this study show that ASS can be used as an effective adsorbent for the elimination of Pb^{2+} , Cu^{2+} , Zn^{2+} , and Ni^{2+} metal ions from aqueous solutions. Better efficacy of ASS adsorbent was observed at optimum parameters like adsorbent dose (4g/100ml), pH (5), temperature (35 °C), shaking time (4h), and shaking speed 220 rpm. PFO, PSO, Langmuir, Freundlich and Temkin all adsorption cases studied. But additionally, adsorption data were well-fitted by PSO kinetics and Langmuir isotherm models.

REFERENCES

1. V. Marcano, P. Benitez, E. Palacios-Prü, *Planet Space Sci*, **51**, 159 (2003).
2. A. Blanco, M. Pignata, H. Lascano, M. Salazar, J. Rodriguez. *Env. Sci. Pollut. Res*, **28**, 20624 (2021).
3. T. Mahmudiono, D. Boko.v, G. Widjaja, I. S. Konstantinov, K. Setiyawan, W. K. Abdelbasset, H.

- S. Majdi, M. M. Kadhim, H. A. Kareem, K. Bansal. *Food Sci. Technol, Campinas*, **42**, e111721 (2022).
4. C. Su, *Environ. Skept. Crit.*, **3**, 24 (2014).
5. A.K. Singh, V. Aggarwal, U. P. Singh, S. Mehtab, *Talanta*, **77**, 718 (2008).
6. A. K. Singh, U. P. Singh, V. Aggarwal, S. Mehtab, *Anal. Bioanal. Chem.*, **391**, 2299 (2008).
7. I. R. Chowdhury, S. Chowdhury, M. A. J. Mazumder, A. Al-Ahmed, *Appl. Water Sci.*, **12**, 185 (2022).
8. M. Tamás, S. Sharma, S. Ibstedt, T. Jacobson, P. Christen, *The National Center for Biotechnology Information (NCBI)*, **4**, 252 (2014).
9. P. Tchounwou, C. Yedjou, A. Patlolla, D. Sutton. *Springer, Berlin*, 2012, p. 133.
10. S. P. Mishra, *Biointerface Research in Appl. Chem.*, **12**, 2, 1884 (2022).
11. S. Ai-Asheh, R. Banat, Ai-omari, Duvnjak. *Chemosphere*, **41**, 659 (2000).
12. K. Vijayaraghavan, S. Yun. *Biotechnology Adv* **26**:266 (2008).
13. N. Gaur, A. Kukreja, M. Yadav, A. Tiwar. *Applied Water Science*, **8**, 98 (2018).
14. S. Najiah, M. Yusoff, A. Kamari, W. P. Putra, C. F. Ishak, A. Mohamed, N. Hashim, I. Md Isa, *Studies. Jour. of Env. Protection*, **5**, 289 (2014).

F. Ummul Khair et al.: Efficient removal of Pb^{2+} , Ni^{2+} , Cu^{2+} , and Zn^{2+} ions from water using activated soybean seed...

15. F. Zhang, B. Zhang, H. Dandan, W. Lishun, H. Wanguo. *Open Chemistry*, **19**, 726 (2021).
16. X. Wei, L. Hui-Ru, L. Wang, H. Yu-Feng, R. Wang. *Pure Appl. Chem*, (2014).
17. J. A. Torres, F. G. E. Nogueira, M. C. Silva, J. H. Lopes, T. S. Tavares, T. C. Ramalho, *RSC Adv.* **7**, 16460 (2017).
18. S.N. Jain, P.R. Gogate. *J Mol Liq.*, **243** (2017).
19. D. Arimurti, E. Heraldy, W. Lestari. in: AIP conference proceedings, Vol 1. AIP Publishing, 2016, p. 030036.
20. L. Khezami, R. Capart. *J. Hazard. Mater.*, **123**, 223 (2005).
21. M. Saleem, T. Pirzada, R. Qadeer. *Colloids Surf. A*, **292**, 246 (2007).
22. Z. Hu, H. Chen, S. Yuan. *J. of Hazardous Materials*, **173**, 292 (2010).
23. A.K. Singh, A.K. Jain, P. Saxena, S. Mehtab, *Electroanalysis*, **18 (12)**, 1186 (2006).
24. A. Heidari, H. Younesi, Z. Mehraban, H. Heikkinen. *International Jour. of Biological Macromolecules*, **61**, 251 (2013).
25. Renu, M. Agarwal, K. Singh. *J Water Reuse Desalin.*, **7(4)**, 387 (2017).
26. A.K. Singh, S. Mehtab, U. P. Singh, V. Aggarwal, *Anal. Bioanal. Chem.*, **388 (8)**, 1867 (2007).
27. A.K. Singh, S. Mehtab, A.K. Jain, *Anal. Chim. Acta* **575 (1)**, 25 (2006).
28. J.S. Yadav, M. Soni, A. Lashkari, *International Refereed Jour. of Eng. and Sci.*, **6**, 30 (2017).